NIH Public Access
Author Manuscript
J Neurosci Res. Author manuscript; available in PMC 2014 August 11.

Published in final edited form as:
J Neurosci Res. 2011 October ; 89(10): 1531–1541. doi:10.1002/jnr.22684.

Slit-Robo Signals Regulate Pioneer Axon Pathfinding of the Tract of the Postoptic Commissure in the Mammalian Forebrain

Itzel Ricaño-Cornejo[1], **Amy L. Altick**[2], **Claudia M. García-Peña**[1], **Hikmet Feyza Nural**[2], **Diego Echevarría**[3], **Amaya Miquelajáuregui**[1], **Grant S. Mastick**[2], and **Alfredo Varela-Echavarría**[1,*]

[1]Instituto de Neurobiología, Universidad Nacional Autónoma de México, Querétaro, México

[2]Department of Biology, University of Nevada, Reno, Nevada

[3]Instituto de Neurociencias, Universidad Miguel Hernández, Alicante, Spain

Abstract

During early vertebrate forebrain development, pioneer axons establish a symmetrical scaffold descending longitudinally through the rostral forebrain, thus forming the tract of the postoptic commissure (TPOC). In mouse embryos, this tract begins to appear at embryonic day 9.5 (E9.5) as a bundle of axons tightly constrained at a specific dorsoventral level. We have characterized the participation of the Slit chemorepellants and their Robo receptors in the control of TPOC axon projection. In E9.5–E11.5 mouse embryos, Robo1 and Robo2 are expressed in the nucleus origin of the TPOC (nTPOC), and Slit expression domains flank the TPOC trajectory. These findings suggested that these proteins are important factors in the dorsoventral positioning of the TPOC axons. Consistently with this role, Slit2 inhibited TPOC axon growth in collagen gel cultures, and interfering with Robo function in cultured embryos induced projection errors in TPOC axons. Moreover, absence of both Slit1 and Slit2 or Robo1 and Robo2 in mutant mouse embryos revealed aberrant TPOC trajectories, resulting in abnormal spreading of the tract and misprojections into both ventral and dorsal tissues. These results reveal that Slit-Robo signaling regulates the dorsoventral position of this pioneer tract in the developing forebrain.

Keywords

knockout mouse; axonal projections; brain development; calbindin; axonal growth

Discrete sources of guidance cues in the developing brain control axon growth along longitudinal routes and orchestrate the formation of complex pathways (Erskine et al., 2000; Bagri et al., 2002; Hernandez-Montiel et al., 2003, 2008). In vertebrates, the earliest scaffold of longitudinal axons to form during forebrain development is the tract of the postoptic commissure (TPOC). The relevance of this tract as a pioneer pathway has been revealed by its ablation in *Xenopus* embryos, which causes aberrant projection of the supraoptic tract

© 2011 Wiley-Liss, Inc.

*Correspondence to: Alfredo Varela-Echavarría, Instituto de Neurobiologia-UNAM, Blvd. Juriquilla 3001, Queretaro, Qro., Mexico 76230. avarela@unam.mx or Grant S. Mastick, Department of Biology, University of Nevada, Reno NV 89557. gmastick@unr.edu.
I. Ricaño-Cornejo and A.L. Altick contributed equally to this work.

Additional Supporting Information may be found in the online version of this article.

NIH-PA Author Manuscript
NIH-PA Author Manuscript
NIH-PA Author Manuscript

NIH-PA Author Manuscript

NIH-PA Author Manuscript

NIH-PA Author Manuscript

(Anderson and Key, 1996) and of retinal axons (Taylor, 1991). Moreover, in zebrafish, its absence affects the pathfinding of axons from the nucleus of the posterior commissure at two different choice points (Chitnis et al., 1992).

As in other vertebrate embryos, the TPOC is the earliest tract to form in the mouse diencephalon. On E9.5, TPOC axons emerge from a neuronal nucleus located rostral and ventral to the optic stalk (Easter et al., 1993; Mastick and Easter, 1996). By E10, the tract has extended through the ventral aspect of the diencephalic alar plate, where it merges with other early longitudinal axon bundles (Nural and Mastick, 2004). By E11.5, the tract reaches the midbrain and merges with the tract of the mesencephalic nucleus of the trigeminal nerve. The TPOC is conserved in vertebrate evolution; in all vertebrate embryos examined, including mouse, *Xenopus* (Anderson and Key, 1999), zebrafish (Ross et al., 1992), and chick (Chedotal et al., 1995), the tract originates and extends longitudinally from the rostralmost part of the lamina terminalis in the forebrain to the hindbrain.

Little is known about the molecular control of TPOC axon projection during embryonic development. In *Xenopus*, the study of TPOC axon projection has been directed mainly at the formation of its ventral commissure in the midbrain, which is impaired by degrading chondroitin sulfate, blocking neuropilin-1 expression (Anderson et al., 1998, 2000b), or blocking DCC-dependent interactions in TPOC axons (Anderson et al., 2000a). In zebrafish embryos, interference with Slit or Robo function causes reduction in TPOC fasciculation in the posterior forebrain (Devine and Key, 2008).

Slit proteins have been described as chemorepellent molecules for a large variety of neuronal groups and axons, including various populations in the forebrain (Brose et al., 1999; Nguyen-Ba-Charvet et al., 1999, 2004; Erskine et al., 2000; Bagri et al., 2002). To date, three distinct vertebrate *Slit* genes have been identified, and all are expressed in the CNS (Holmes et al., 1998; Itoh et al., 1998; Brose et al., 1999; Li et al., 1999; Marillat et al., 2002). In addition, the expression of three members of the Slit receptor family, the Robo proteins, has been well characterized in the vertebrate CNS (Lee et al., 2001; Marillat et al., 2002; Camurri et al., 2004; Sundaresan et al., 2004; Lopez-Bendito et al., 2007). In the present work, we studied the expression and function of Robo and Slit proteins in the early stages of TPOC axon projection in mouse embryos. Our results reveal that Slit-Robo signaling participates in the control of TPOC axon projection by regulating its dorsoventral position along the ventral forebrain.

MATERIALS AND METHODS

Animals

CD-1 mouse embryos (*Mus musculus*) were used for in situ hybridization, whole brain cultures, and immunohistochemistry. The day of the vaginal plug was considered as embryonic day (E) 0.5. For in situ hybridization and immunohistochemistry, embryos were fixed in 3.5% paraformaldehyde (PFA) in PBS and stored at 4°C. Animals were handled humanely according to regulations of the Mexican government (NOM-062-ZOO-1999) and following the *Guide for the care and use of laboratory animals* (Institute of Laboratory Animal Resources, NRC). For knockout studies we used *Slit1/2* double mutants, which were

NIH-PA Author Manuscript

NIH-PA Author Manuscript

NIH-PA Author Manuscript

offspring of *Slit1*$^{-/-}$;*Slit2*$^{+/-}$ heterozygotes, interbred with each other for six to 10 generations. *Robo1*, *Robo2*, and *Robo1/2* mutant mice were maintained as heterozygotes back-crossed to CD1 outbred wild-type mice for six to 10 generations. *Slit1/2*, *Robo1*, *Robo2*, and *Robo1/2* mice were a kind gift from Marc Tessier-Lavigne (Genentech Inc., South San Francisco, CA; Grieshammer et al., 2004; Long et al., 2004; Lopez-Bendito et al., 2007). Animals were maintained according to UNR IACUC protocols, following NIH guidelines.

Immunohistochemistry

For fluorescent immunostaining, whole embryos were fixed, cryoprotected with sucrose, and crysectioned. Horizontal 12-μm sections collected on slides were stained with Robo1 and Robo2 rabbit antibodies (see Fig. 2A,B; 5 and 10 ng/ml, respectively; Long et al., 2004). Detection was performed with secondary antibodies labeled with Cy3 (anti-rabbit; Invitrogen, Carlsbad, CA). For whole-brain immunostaining, fixed embryos were washed extensively in PBS. Brains were dissected out and incubated for 2 hr in PBS with 0.3% Triton X-100 and 0.5% goat serum, for 24 hr in the same solution containing antibodies for β-tubulin III (mouse, 1:1,000, E7; Developmental Studies Hybridoma Bank, Iowa City, IA), Robo1 (mouse, 1:250, WH000609; Sigma-Aldrich, St. Louis, MO; Fig. 2D,E), or calbindin-D28K (rabbit, 1:1,000, AB1778; Chemicon, Millipore, Billerica, MA); washed extensively with PBS; and incubated with Cy3 or Alexa 483 fluoresent secondary antibodies in PBS (Invitrogen) followed by extensive washing. Brains were cut along the dorsal and the ventral midline, and hemibrains were mounted pial-side-up on coverslips for image capture in a confocal Nikon Y-FL microscope using an He-Ne (emission 543 nm) laser and an argon laser (emission 488 nm). Specificity of the Robo1 Sigma-Aldrich antibody was confirmed by immunodetection of the axons emanating from the mammillary region in whole brains previously shown to express Robo1 and not Robo2 (Marion et al., 2005; Farmer et al., 2008; Tsuchiya et al., 2009).

Whole-Mount In Situ Hybridization

The expression patterns of *Slit1*, *Slit2*, *Slit3*, *Robo1*, and *Robo2* were determined in CD-1 mouse embryos embryos, using digoxigenin-labeled antisense probes (kindly provided by Dr. Marc Tessier-Lavigne). Whole-mount in situ hybridization was performed as described by Wilkinson (1992).

Whole Mouse Embryo Cultures

Pregnant CD1 mice were killed by cervical dislocation, and embryos were cultured as described elsewhere (de Carlos et al., 1996). The cultures were maintained for 24 hr at 368C with 95%O_2-5% CO_2 in the presence of 20 ng/ml each of Fc protein chimeras containing the extracellular domain of Robo1 or Robo2 or of 40 ng/ml of control IgG-Fc proteins (1749-RB-050, 3147-RB-050, 110-HG; R&D Systems, Minneapolis, MN). Activity of Robo1 and Robo2 chimeras was confirmed, in that they inhibited axon growth of embryonic dopaminergic axons known to respond to Slit proteins (Lin et al., 2005; Dugan et al., 2011). After incubation, embryos were fixed with 4% PFA for at least 2 hr, followed by immunostaining as described above.

NIH-PA Author Manuscript

NIH-PA Author Manuscript

NIH-PA Author Manuscript

Explant Outgrowth Assays

E10.5 mouse brain tissue was dissected in ice-cold DMEM medium from the base of the optic stalk, removing mesenchyme and epidermis. COS cells were transfected by lipofection of a Slit2-myc (Brose et al., 1999) or a GFP-expressing vector, cultured for 24 hr, and aggregated in a hanging drop of media. Transfection was monitored either by GFP fluorescence in control aggregates or by immunostaining with anti-myc antibodies. TPOC tissue and COS cell aggregates were then arranged on a drop of liquid collagen and allowed to gel, followed by culture for 2–3 days in DMEM containing 10% fetal bovine serum. The explants were then fixed with 4% PFA, and labelled sequentially with the neuron-specific β-tubulin III and fluorescent secondary antibodies. The nTPOC is the only neuronal nucleus in this brain area at this stage, so only TPOC axons are expected to grow from these explants. Outgrowth was quantified (straight line measurement in ImageJ; NIH) in images of the explants by measuring the length of each neurite or bundle within the two quadrants either toward or away from the COS cell aggregate. For each explant, neurite lengths were summed within each quadrant, and the ratio between toward and away growth was calculated. Student's *t*-test was used to compare the mean ratios between control GFP and Slit2 transfections.

Analysis of Mutant Mouse Embryos

Slit double mutants were generated from crosses between *Slit1*$^{-/-}$;*Slit2*$^{+/-}$ or *Slit1*$^{+/-}$;*Slit2*$^{+/-}$ mice. Slit2 mutants were generated by crosses of *Slit1*$^{++}$;*Slit2*$^{+/-}$ mice. Robo double mutants were maintained as a *Robo1*$^{+/-}$;*Robo2*$^{+/-}$ line. Embryos were genotyped by PCR (Grieshammer et al., 2004). Homozygous wild-type or heterozygote littermates were used as controls. Embryos were collected at embryonic day E10.5 (noon of the day of the vaginal plug was designated as E0.5). Embryos were fixed in 4% paraformaldehyde in 0.1 M phosphate buffer at 48°C. The lipophilic fluorescent dye DiI was used for tracing of axons in control and mutant embryos as previously described (Mastick and Easter, 1996; Nural and Mastick, 2004). The numbers of embryos of each genotype analyzed (almost all labelled bilaterally with similar TPOC trajectories) were *Slit1*$^{+/+}$;*Slit2*$^{+/+}$, n=2; *Slit1*$^{+/+}$;*Slit2*$^{+/-}$, n=1; *Slit1*$^{+/+}$;*Slit2*$^{-/-}$, n=3; *Slit1*$^{+/-}$;*Slit2*$^{+/+}$, n=2; *Slit1*$^{+/-}$;*Slit2*$^{+/-}$, n=6; *Slit1*$^{+/-}$;*Slit2*$^{-/-}$, n=4; *Slit1*$^{-/-}$;*Slit2*$^{+/+}$, n=3; *Slit1*$^{-/-}$;*Slit2*$^{+/-}$, n=6; *Slit1*$^{-/-}$;*Slit2*$^{-/-}$, n=5; *Robo1*$^{+/+}$; *Robo2*$^{+/-}$, n=6; *Robo1*$^{+/+}$;*Robo2*$^{-/-}$, n=5; *Robo1*$^{+/-}$;*Robo2*$^{+/+}$, n=4; *Robo1*$^{+/-}$;*Robo2*$^{+/-}$, n=3; *Robo1*$^{-/-}$;*Robo2*$^{+/+}$, n=6; and *Robo1*$^{-/-}$;*Robo2*$^{-/-}$, n=5.

RESULTS

Expression of Slit1 and Slit2 and Their Receptors Robo1 and Robo2 Suggests a Role in TPOC Axon Pathfinding

To identify guidance cues that could be involved in determining the trajectory of TPOC axons, we examined the expression of *Slit1*, *Slit2*, and *Slit3* and that of their receptors *Robo1* and *Robo2* during mouse stages when the TPOC projection is being established. We found that *Slit1* and *Slit2*, but not *Slit3*, are expressed in the ventral aspect of the developing forebrain from E9.5 to E11.5, in patterns that suggest their participation in TPOC formation. From E9.5 onward, *Slit1* mRNA was detected in ventral and caudal sides of the optic stalk and in a continuous ventral band spanning the caudal diencephalon, midbrain, and hindbrain

NIH-PA Author Manuscript

NIH-PA Author Manuscript

NIH-PA Author Manuscript

(Fig. 1A–D). At E9.5, expression of *Slit2* in the caudal diencephalon and in the midbrain resembled that of *Slit1*, but occupying a more compact and ventral domain, and it was also found in the preoptic region rostral and dorsal to the optic stalk (Fig. 1E). At E10.5 and E11.5, *Slit2* was additionally expressed in a ventral domain in the whole rostrocaudal extent of the diencephalon (Fig. 1F–H) and in E11.5 around the optic stalk. Notably, at E9.5 and E10.5, a gap that coincides with the location of the nTPOC (arrowhead in all figures) was observed between the pre-optic and the ventral diencephalic *Slit2* domains. *Slit3* expression was not detected in the diencephalon at the stages studied, but it was detected in the ventral region of the midbrain, hindbrain, and spinal cord (Supp. Info. Fig. 1), as previously described (Yuan et al., 1999).

We also analyzed the expression in the developing mouse forebrain of the known Slit receptors, *Robo1* and *Robo2*. By in situ hybridization, we found that both genes are expressed in the region that harbors TPOC neurons (arrowhead), in a partially complementary pattern to that of *Slits*. From E9.5 to 11.5, *Robo1* was found ventral and rostral to the optic stalk (Fig. 1I–L). Similar results were obtained for *Robo2* (Fig. 1M–P). To confirm the presence of Robo proteins in TPOC neurons, we performed immunostaining on coronal sections of E10.5 mouse embryos using antibodies for Robo1 and Robo2 (Long et al., 2004) and detected staining at a region adjacent and ventral to the optic stalk (Fig. 2A,B). Moreover, whole-brain immunostaining of E11.5 embryos with a Robo1 antibody revealed the presence of a prominent axon bundle in the same region that was also labelled specifically with an antibody for the EF-hand protein calbindin (CB; Fig. 2C–E). At these stages only TPOC axons are found in this region (Mastick and Easter, 1996), so these results indicate that TPOC neurons possess Robo receptors and may be able to respond to Slits. The results of the expression studies suggest that Slit1 and Slit2 are in a position to first steer Robo-expressing TPOC axons out of the base of the optic stalk, preventing dorsal and ventral growth while Slit2 prevents ventral growth in the caudal diencephalon.

Slit2 Inhibits TPOC Axon Growth

Given the potential of Robo1/2-expressing TPOC neurons to respond to Slits and taking into account the expression pattern of *Slit2* in regions flanking the TPOC, we tested the effect of Slit2 on TPOC axonal growth in collagen gel cultures. For this, we isolated neuroepithelial explants from E10.5 mouse embryos containing the nTPOC and cultured them adjacent either to COS cell aggregates expressing Slit2-myc or to control aggregates (untransfected or transfected with an expression vector for green fluorescent protein; GFP). After culture for 24 hr, axons were immunostained, and their lengths measured. The ratio of axon growth in the quadrant facing the cell aggregate to that of the opposite quadrant was obtained for control (GFP; Fig. 3A) or Slit2-expressing aggregates (Fig. 3B). A statistically significant inhibitory effect of Slit2 on TPOC axon growth was detected compared with control GFP-expressing and untransfected COS cell aggregates (Fig. 3C, and data not shown). These results indicate a direct inhibitory effect of Slit2 on TPOC axons in vitro, consistent with the role suggested by its expression in the developing forebrain.

NIH-PA Author Manuscript

NIH-PA Author Manuscript

NIH-PA Author Manuscript

Impairing Robo Function Induces Aberrant TPOC Projection in Cultured Embryos

Immunostaining of E9.5 mouse embryos with the CB antibody allowed visualization of the nucleus of origin of the TPOC, the nTPOC, at the rostral and ventral edges of the optic stalk (not shown). At E10, CB-expressing axons projected a short distance caudal to the optic stalk, following a route through the diencephalon resembling closely the TPOC projection previously described using antibodies for β-tubulin III (TuJ-1) and lipophilic tracers (Fig. 4A; Easter et al., 1993; Mastick and Easter, 1996). These results, and those shown in Figure 2C, indicate that CB is a reliable marker for TPOC axons in mouse embryos at their early stages of projection.

To study the role of Slit/Robo signaling in the establishment of the TPOC projection, we performed whole-embryo culture experiments in the presence of control IgG-Fc or of Robo-Fc protein chimeras to block Robo/Slit signalling. In control E9.5 embryos cultured for 24 hr in the presence of IgG-Fc chimeras, TPOC axons revealed by CB immunostaining were detected coursing ventral to the optic stalk and into the caudal diencephalon (Fig. 4B; n = 4) following a normal pathway. Hence, the culture system employed reproduces the initial phases of the TPOC projection following the route predicted from the pathway observed in vivo.

In embryos cultured for 24 hr in the presence of Robo1 and Robo2-Fc chimeras, TPOC axons projected abnormally around the optic stalk in a dorsal direction (Fig. 4C; n = 6). Other TPOC axons in the same embryos, however, followed the normal caudal direction after an abnormal dorsal detour caudal to the optic stalk (arrow in Fig. 4C). To assess alterations to the overall distribution of axon tracts in the ventral diencephalic region, IgG-Fc- and Robo-Fc-treated cultures were stained for β-tubulin III. Axon bundles of similar appearance were detected in the ventral diencephalon, and no gross abnormalities were detected in either type of culture (Fig. 4D,E), indicating that the effects of the Robo-soluble proteins were specific for TPOC axons.

Robo1 and Robo2 Are Required for TPOC Navigation

Robo expression in TPOC neurons suggests a role in TPOC axon navigation through the forebrain. As a complementary approach to the explant and whole embryo culture experiments, we tested Robo function by analyzing TPOC projections in Robo1, Robo2, and Robo1/2 knockout embryos by placing DiI crystals in the nTPOC to label anterogradely growing axons (arrowhead in Fig. 5A).

Embryos lacking all four alleles of Robo, i.e., *Robo1/2* double mutants, had severe guidance defects (Fig. 5D). The initial axon projections were as in wild-type embryos, with fibers growing posteriorly in a fascicle past the optic stalk and then fanning out slightly as they projected through the diencephalon to transit the thalamus. In *Robo1/2* mutants, a subset of axons diverged abnormally around the optic stalk (Fig. 5D,F), turning dorsally into the preoptic region, as observed in embryos cultured in the presence of Robo soluble proteins. Many of the *Robo1/2* double mutant axons projected farther into the diencephalon, but most

NIH-PA Author Manuscript

NIH-PA Author Manuscript

NIH-PA Author Manuscript

fanned out widely. A subset veered ventrally toward and across the midline of the hypothalamus (Fig. 5E), a phenotype never seen in wild-type embryos. An additional group of errant axons projected abnormally into the dorsal thalamus, essentially failing to make the normal turn toward the midbrain (Fig. 5D).

To assess a potential functional redundancy between Robo1 and Robo2, single Robo mutants were also examined. Although loss of *Robo1* resulted in a wild-type pattern (Fig. 5B), loss of *Robo2* affected a subset of embryos (two of five) in which the tract widened as the axons passed through the thalamus (Fig. 5C). This $Robo2^{-/-}$ phenotype, however, was less severe than that of *Robo1/2* double mutants, insofar as no drastic errors were seen either around the optic stalk or toward the ventral midline.

Additional labels were made on embryos with other combinations of *Robo1* and *Robo2* alleles, i.e., those lacking one, two, or three of the wild-type alleles (total n = 24 in all genotypes; described in Materials and Methods). The majority of these (15 of 24) had TPOC projections indistinguishable from wild type. In a minority, widening similar to that of $Robo2^{-/-}$ embryos was seen with other *Robo* allele combinations, including those missing only one *Robo* allele (three of 10 that were either $Robo1^{+/-}$;$Robo2^{+/+}$ or $Robo1^{+/+}$;$Robo2^{+/-}$) or missing two Robo alleles (one of three $Robo1^{+/-}$;$Robo2^{+/-}$). In the remaining embryos analyzed (five of 24, consisting of three $Robo1^{+/-}$;$Robo22^{+/-}$, one $Robo2^{-/-}$, and one $Robo1^{+/+}$;$Robo22^{+/-}$), a few axons (two to six) made dorsal projections around the optic stalk. Hence, compared with the complete penetrance and more severe errors observed in *Robo1/2* double mutants, this analysis suggests that either *Robo1* or *Robo2* is sufficient to guide most TPOC axons into and through the diencephalon.

To determine whether the abnormalities observed in TPOC axons were specific or secondary to alterations to other axon tracts, control and Robo double mutant brains were stained for β-tubulin III (Fig. 5K–N). No gross abnormalities were observed in the double mutants except for some dorsally wandering axons in the caudal region of the diencephalon resembling those detected by DiI labeling from the nTPOC. These results indicate that the projection errors of TPOC axons are not secondary to gross alterations of other preexisting diencephalic axon tracts.

Slit1 and Slit2 Are Required for TPOC Guidance

To test the function of Slits in guiding TPOC axons, we analyzed single *Slit1* and *Slit2* homozygous mutants as well as mutants carrying various combinations of *Slit1* and *Slit2* mutant alleles (description in Materials and Methods). Overall, *Slit1* mutants had a normal TPOC (Fig. 5G). *Slit2* appeared to have a more important role, insofar as mutants carrying *Slit2* mutant alleles had severe errors, particularly when combined with *Slit1* mutations (Fig. 5H,I, and as described below). In *Slit1/2* double mutants, TPOC axons made severe pathfinding errors, straying both ventrally and dorsally (Fig. 5J). These mutants (five of five) showed TPOC errors similar to the *Robo1/2* double mutants, namely, projection around the optic stalk, and axons that grew toward and across the ventral midline. Axons that projected posteriorly fanned out widely as well. Likely as a result of the turning errors, the tract in *Slit1/2* double mutants appeared shorter than in age-matched controls, particularly at E11 (not shown).

NIH-PA Author Manuscript

NIH-PA Author Manuscript

NIH-PA Author Manuscript

Slit2$^{-/-}$ mutants also tended to have severe ventral and dorsal errors, although with a reduced penetrance compared with double mutants, which implies a partial redundancy with *Slit1*. Two of three *Slit2*$^{-/-}$ mutants analyzed had severe guidance errors (Fig. 5I) similar to those of *Slit* or *Robo* double mutants (the remaining *Slit2*$^{-/-}$ mutant had a TPOC that appeared normal, though sparse).

In other combinations of Slit mutant alleles, reduced penetrance and mild phenotypes were observed, including dorsal and ventral misprojection and a moderate posterior widening (10 of 20 embryos). In embryos lacking one allele of each *Slit1* and *Slit2* (*Slit1*$^{+/-}$; *Slit2*$^{+/-}$), some axons turned dorsally around the optic stalk (Fig. 5H). Among the subset analyzed that was missing three of four Slit alleles, i.e., *Slit1*$^{-/-}$;*Slit2*$^{+/-}$ or *Slit1*$^{+/-}$;*Slit2*$^{-/-}$, some had axons wandering ventrally or dorsally, though not as many or as far as *Slit1/2* double mutants (five of eight showed this mild wandering; three of eight were normal). Taken together, both *Slit* and *Robo* mutant phenotypes indicate that *Slit/Robo* signals are required for accurate TPOC pathfinding, channeling this tract caudally through the diencephalon, and that *Slit2* plays a more important role in channeling the TPOC than *Slit1*.

DISCUSSION

We present evidence from expression and functional studies that reveals a role for the Slit-Robo guidance system in control of the pioneer TPOC axon projection. *Slit1* and *Slit2* expression domains in the rostral forebrain flank the trajectory of the TPOC during its projection through this region (E9.5–E11). Additionally, *Slit2* flanks the tract on its ventral side throughout the diencephalon. These findings are, in general, in agreement with those reported for mouse and chick embryos (Holmes et al., 1998; Li et al., 1999). The mRNAs of *Robo1* and *Robo2*, the Slit receptors, were detected in mouse embryos in the region containing the nTPOC. This pattern also appears to be conserved; *Robo1* and *Robo2* were found in equivalent regions in zebrafish embryos (Lee et al., 2001). The presence of Robo proteins in TPOC neurons was confirmed by immunostaining in E10.5 and E11.5 mouse embryos. Based on the known repellent effects of Slit molecules mediated by Robo, we anticipated that Slit1and Slit2 would first mediate repulsion of TPOC axons from the base of the optic stalk, preventing their dorsal and ventral growth, whereas Slit2 would prevent ventral growth in the caudal diencephalon.

Slit2 inhibited the growth of TPOC axons in collagen gel cultures. These results reveal that TPOC axons are capable of responding to Slit2 and suggest that Slit-Robo signaling guides TPOC axons, preventing them from entering ventral and rostrodorsal territories in the diencephalon.

Consistently with a role for Slit molecules in guiding TPOC axons, impairing Robo signaling with soluble versions of Robo1 and Robo2 in cultured embryos caused TPOC pathfinding errors. TPOC axons misprojected dorsally into a region that expressed Slit1 at early stages and later also Slit2. In our manipulations in culture, however, no aberrant TPOC axon projection into ventral territories was detected. This could be the result of incomplete blockage of Robo signaling in combination with the observed high expression levels of Slit2 in this region.

NIH-PA Author Manuscript

NIH-PA Author Manuscript

NIH-PA Author Manuscript

To study further the role of Slit-Robo signaling in TPOC axon pathfinding, we analyzed the TPOC projection in *Robo* or Slit mutant embryos. With the double *Robo1/Robo2* mutants, we observed a widely defasciculated tract and two additional phenotypes. First, a few axons turned aberrantly toward the ventral hypothalamic region, and some of them even crossed the midline, which was not observed in wild-type or heterozygous embryos. Second, some axons projected dorsally around the caudal edge of the optic stalk. Analysis of the TPOC on *Slit1/ Slit2* double mutant embryos revealed phenotypes similar to those observed in *Robo* mutants. The finding that these phenotypes were also present in *Slit2* single mutants, albeit with a reduced penetrance, whereas *Slit1* single mutants were normal, suggests a predominant role for *Slit2* in TPOC axon pathfinding. Moreover, the dorsal projection around the optic stalk in *Robo* and *Slit* double mutants and in *Slit2* single mutants is consistent with similar misprojection patterns observed upon impairing Slit-Robo signaling in cultured embryos.

Since no consistent abnormalities were detected in single *Robo* mutant embryos, our overall conclusion is that the two Robos are largely redundant. In contrast, whereas *Slit1* appears to be dispensable in the presence of *Slit2*, the latter has unique functions in determining the stereotypical TPOC axon projection. These findings, in combination with the observed inhibitory effects and the expression pattern of Slit2, suggest that this guidance cue plays a prominent role in TPOC axon pathfinding in the forebrain upon binding Robo1 and Robo2.

Our results show that Slit1 and Slit2 participate in the dorsoventral positioning of the TPOC during its initial projection, channeling it into a caudally directed pathway and preventing axon spreading into ventral and dorsal areas. A similar mechanism has been suggested for Slit1 in the developing thalamus (Bagri et al., 2002). Recent studies also indicate a role for Slit-Robo signaling in dorsoventral positioning of longitudinal dopaminergic axons in mice (Farmer et al., 2008; Kastenhuber et al., 2009; Mastick et al., 2010) and TPOC axons in the zebrafish forebrain (Devine and Key, 2008). In the latter model, a Robo2-mediated Slit1a signal appears to promote axon spreading at the caudal diencephalon, followed by additional signals mediated by Robo1 and Robo3 that prevent further spreading in this region and in the midbrain. Although these findings reveal an overall conserved role in fish and mammals of Slit-Robo signaling in regulating TPOC axon projection, in the latter it does not appear to be involved in inducing spreading of TPOC axons. Moreover, knockdown of Slit1a, Robo1/2, or Robo2/3 in zebrafish embryos caused projection defects only in the caudal region of the diencephalon and did not cause misprojection into the preoptic and supraoptic areas or into the ventral forebrain as observed in mouse mutants. Prominent expression of Slit2 throughout the zebrafish rostral forebrain ventral region (Yeo et al., 2001) might have prevented such projection errors, but the expression of this protein was not manipulated and simultaneous knockdown of all Robo proteins was not analyzed.

Closer to the zebrafish phenotypes were the dorsal deviations of the TPOC in the thalamus in *Robo* and *Slit* mouse mutants. These dorsal and posterior deviations may be analogous to the dorsal spreading by zebrafish TPOC axons in the caudal diencephalon upon knocking down Robo1 and Robo3. The mouse axons spread much farther, however, and do not appear to transit Slit-expressing tissue at any point in their pathway, suggesting a distinct mechanism. In fact, the dorsal spreading of mouse TPOC axons in Robo double mutants,

NIH-PA Author Manuscript

NIH-PA Author Manuscript

NIH-PA Author Manuscript

away from the prominent Slit1 and Slit2 expression domains in the ventral posterior forebrain and in Slit double mutants, is not consistent with a repulsive Slit effect. Induction of axon fasciculation by Slit1/2, perhaps involving homophilic or heterophilic Robo–Robo interactions (Hivert et al., 2002; Liu et al., 2004) of TPOC axons, might explain this phenotype. In a separate study of longitudinal pioneers in midbrain and hindbrain, we have documented other dorsal deviations of axons away from Slit sources in Robo and Slit mutants (Farmer et al., 2008; Dugan et al., 2011). The dorsal deviations in the TPOC and other longitudinal axons suggest that Slit/Robo signaling has a role in promoting longitudinal trajectories by favoring fasciculated axon growth as observed for retinal ganglion cell axons (Ringstedt et al., 2000; Plump et al., 2002), although the mechanism for this function remains an important unanswered question.

The findings of our study are also in agreement with previous data that support a role for Slit-Robo signaling in determining the dorsoventral position of the major forebrain longitudinal tracts, such as the corticofugal, corticothalamic, callosal, corticospinal, thalamocortical, and lateral olfactory as well as hippocampal tracts (Nguyen-Ba-Charvet et al., 1999, 2002; Bagri et al., 2002; Lopez-Bendito et al., 2007). Some of these tracts, such as the corticothalamic, corticospinal, and thalamo-cortical, overlap and potentially follow the earlier TPOC tract, suggesting that some later tract errors may be secondary to the early TPOC errors.

Slit/Robo guidance of the TPOC is also likely to depend on TPOC reactions to other guidance cues. For example, TPOC guidance has previously been shown to depend on Pax6 and R-cadherin. In *Pax6* mutant embryos, TPOC axons project into the ventral thalamus and fail to establish the tract (Mastick et al., 1997). The initially tightly fasciculated part of the tract appeared normal in the mutant and widened caudal to the optic stalk as expected, but some pathfinding abnormalities were detected. Several axons misprojected dorsally around the optic stalk and also into the cerebral vesicle, with many axons forming loops, and, in the diencephalon, TPOC axons halted abnormally. Moreover, in a few cases. some axons projected into the ventral territory (Mastick et al., 1997). Altered R-cadherin expression in *Pax6* mutant embryos appears to be responsible in part for the disruption of the TPOC axon trajectories (Andrews and Mastick, 2003; Nural and Mastick, 2004). Hence, in addition to regulating the expression of R-cadherin or other members of the same family that have been related to Robo function (Rhee et al., 2002), *Pax6* could regulate aspects of Slit/Robo signaling, particularly in caudal sections of the TPOC pathway.

In conclusion, we present evidence that links Slit1 and Slit2 signaling through Robo1 and Robo2 to axon guidance of the TPOC. Our data suggest that, in the rostral forebrain, Slits channel TPOC axons within their tract specifying their dorsoventral position. Hence, Slit-Robo signaling is likely to be relevant for the projection of other tracts that use this pioneer tract as scaffold in their route finding.

Acknowledgments

Technical support was provided by Anaid Antaramián, Adriana González, Martín García Servín, Alberto Lara, Omar Hernández, Ramón Martínez, Leonor Casanova, Lourdes Lara, and Nydia Hernández. We thank Constantino Sotelo for insightful comments on the manuscript.

NIH-PA Author Manuscript

NIH-PA Author Manuscript

NIH-PA Author Manuscript

Contract grant sponsor: The Wellcome Trust; Contract grant number: GR071174; Contract grant sponsor: CONACYT; Contract grant number: 101433 (to A.V.-E.); Contract grant sponsor: CONACYT (to I.R.-C. and C.M.G.-P.); Contract grant sponsor: Program Ramón y Cajal-2004, Spanish Ministry of Health, Instituto de Salud Carlos III-CIBERSAM; Contract grant sponsor: MEC; Contract grant number: SAF2008-01004; Contract grant sponsor: NIH; Contract grant number: P20 RR-016464; Contract grant sponsor: INBRE Program of the National Center for Research Resources; Contract grant number: HD38069; Contract grant number: NS054740; Contract grant sponsor: March of Dimes; Contract grant number: 1-FY06-387 (to G.S.M.); Contract grant sponsor: DGAPA-UNAM (to A.M.).

REFERENCES

Anderson RB, Key B. Expression of a novel N-CAM glycoform (NOC-1) on axon tracts in embryonic *Xenopus* brain. Dev Dyn. 1996; 207:263–269. [PubMed: 8922525]

Anderson RB, Key B. Novel guidance cues during neuronal path-finding in the early scaffold of axon tracts in the rostral brain. Development. 1999; 126:1859–1868. [PubMed: 10101120]

Anderson RB, Walz A, Holt CE, Key B. Chondroitin sulfates modulate axon guidance in embryonic *Xenopus* brain. Dev Biol. 1998; 202:235–243. [PubMed: 9769175]

Anderson RB, Cooper HM, Jackson SC, Seaman C, Key B. DCC plays a role in navigation of forebrain axons across the ventral midbrain commissure in embryonic *Xenopus* . Dev Biol. 2000a; 217:244–253. [PubMed: 10625550]

Anderson RB, Jackson SC, Fujisawa H, Key B. Expression and putative role of neuropilin-1 in the early scaffold of axon tracts in embryonic *Xenopus* brain. Dev Dyn. 2000b; 219:102–108. [PubMed: 10974677]

Andrews GL, Mastick GS. R-cadherin is a Pax6-regulated, growth-promoting cue for pioneer axons. J Neurosci. 2003; 23:9873–9880. [PubMed: 14586016]

Bagri A, Marin O, Plump AS, Mak J, Pleasure SJ, Rubenstein JL, Tess-ier-Lavigne M. Slit proteins prevent midline crossing and determine the dorsoventral position of major axonal pathways in the mammalian forebrain. Neuron. 2002; 33:233–248. [PubMed: 11804571]

Brose K, Bland KS, Wang KH, Arnott D, Henzel W, Goodman CS, Tessier-Lavigne M, Kidd T. Slit proteins bind Robo receptors and have an evolutionarily conserved role in repulsive axon guidance. Cell. 1999; 96:795–806. [PubMed: 10102268]

Camurri L, Mambetisaeva E, Sundaresan V. Rig-1 a new member of Robo family genes exhibits distinct pattern of expression during mouse development. Gene Expr Patterns. 2004; 4:99–103. [PubMed: 14678835]

Chedotal A, Pourquie O, Sotelo C. Initial tract formation in the brain of the chick embryo: selective expression of the BEN/SC1/DM-GRASP cell adhesion molecule. Eur J Neurosci. 1995; 7:198–212. [PubMed: 7757257]

Chitnis AB, Patel CK, Kim S, Kuwada JY. A specific brain tract guides follower growth cones in two regions of the zebrafish brain. J Neurobiol. 1992; 23:845–854. [PubMed: 1431848]

de Carlos JA, Lopez-Mascaraque L, Valverde F. Dynamics of cell migration from the lateral ganglionic eminence in the rat. J Neurosci. 1996; 16:6146–6156. [PubMed: 8815897]

Devine CA, Key B. Robo-Slit interactions regulate longitudinal axon pathfinding in the embryonic vertebrate brain. Dev Biol. 2008; 313:371–383. [PubMed: 18061159]

Dugan JP, Stratton A, Riley HP, Farmer WT, Mastick GS. Midbrain dopaminergic axons are guided longitudinally through the diencephalon by Slit/Robo signals. Mol Cell Neurosci. 2011; 46:347–356. [PubMed: 21118670]

Easter SS Jr, Ross LS, Frankfurter A. Initial tract formation in the mouse brain. J Neurosci. 1993; 13:285–299. [PubMed: 8423474]

Erskine L, Williams SE, Brose K, Kidd T, Rachel RA, Goodman CS, Tessier-Lavigne M, Mason CA. Retinal ganglion cell axon guidance in the mouse optic chiasm: expression and function of robos and slits. J Neurosci. 2000; 20:4975–4982. [PubMed: 10864955]

Farmer WT, Altick AL, Nural HF, Dugan JP, Kidd T, Charron F, Mastick GS. Pioneer longitudinal axons navigate using floor plate and Slit/Robo signals. Development. 2008; 135:3643–3653. [PubMed: 18842816]

NIH-PA Author Manuscript

NIH-PA Author Manuscript

NIH-PA Author Manuscript

Grieshammer U, Le M, Plump AS, Wang F, Tessier-Lavigne M, Martin GR. SLIT2-mediated ROBO2 signaling restricts kidney induction to a single site. Dev Cell. 2004; 6:709–717. [PubMed: 15130495]

Hernandez-Montiel HL, Melendez-Herrera E, Cepeda-Nieto AC, Mejia-Viggiano C, Larriva-Sahd J, Guthrie S, Varela-Echavarria A. Diffusible signals and fasciculated growth in reticulospinal axon pathfinding in the hindbrain. Dev Biol. 2003; 255:99–112. [PubMed: 12618136]

Hernandez-Montiel HL, Tamariz E, Sandoval-Minero MT, Varela-Echavarria A. Semaphorins 3A, 3C, and 3F in mesencephalic dopaminergic axon pathfinding. J Comp Neurol. 2008; 506:387–397. [PubMed: 18041777]

Hivert B, Liu Z, Chuang CY, Doherty P, Sundaresan V. Robo1 and Robo2 are homophilic binding molecules that promote axonal growth. Mol Cell Neurosci. 2002; 21:534–545. [PubMed: 12504588]

Holmes GP, Negus K, Burridge L, Raman S, Algar E, Yamada T, Little MH. Distinct but overlapping expression patterns of two vertebrate slit homologs implies functional roles in CNS development and organogenesis. Mech Dev. 1998; 79:57–72. [PubMed: 10349621]

Itoh A, Miyabayashi T, Ohno M, Sakano S. Cloning and expressions of three mammalian homologues of *Drosophila* slit suggest possible roles for Slit in the formation and maintenance of the nervous system. Brain Res Mol Brain Res. 1998; 62:175–186. [PubMed: 9813312]

Kastenhuber E, Kern U, Bonkowsky JL, Chien CB, Driever W, Schweitzer J. Netrin-DCC, Robo-Slit, and heparan sulfate proteoglycans coordinate lateral positioning of longitudinal dopaminergic diencephalospinal axons. J Neurosci. 2009; 29:8914–8926. [PubMed: 19605629]

Lee JS, Ray R, Chien CB. Cloning and expression of three zebrafish roundabout homologs suggest roles in axon guidance and cell migration. Dev Dyn. 2001; 221:216–230. [PubMed: 11376489]

Li HS, Chen JH, Wu W, Fagaly T, Zhou L, Yuan W, Dupuis S, Jiang ZH, Nash W, Gick C, Ornitz DM, Wu JY, Rao Y. Vertebrate slit, a secreted ligand for the transmembrane protein roundabout, is a repellent for olfactory bulb axons. Cell. 1999; 96:807–818. [PubMed: 10102269]

Lin L, Rao Y, Isacson O. Netrin-1 and slit-2 regulate and direct neurite growth of ventral midbrain dopaminergic neurons. Mol Cell Neurosci. 2005; 28:547–555. [PubMed: 15737744]

Liu Z, Patel K, Schmidt H, Andrews W, Pini A, Sundaresan V. Extracellular Ig domains 1 and 2 of Robo are important for ligand (Slit) binding. Mol Cell Neurosci. 2004; 26:232–240. [PubMed: 15207848]

Long H, Sabatier C, Ma L, Plump A, Yuan W, Ornitz DM, Tamada A, Murakami F, Goodman CS, Tessier-Lavigne M. Conserved roles for Slit and Robo proteins in midline commissural axon guidance. Neuron. 2004; 42:213–223. [PubMed: 15091338]

Lopez-Bendito G, Flames N, Ma L, Fouquet C, Di Meglio T, Chedotal A, Tessier-Lavigne M, Marin O. Robo1 and Robo2 cooperate to control the guidance of major axonal tracts in the mammalian fore-brain. J Neurosci. 2007; 27:3395–3407. [PubMed: 17392456]

Marillat V, Cases O, Nguyen-Ba-Charvet KT, Tessier-Lavigne M, Sotelo C, Chedotal A. Spatiotemporal expression patterns of slit and robo genes in the rat brain. J Comp Neurol. 2002; 442:130–155. [PubMed: 11754167]

Marion JF, Yang C, Caqueret A, Boucher F, Michaud JL. Sim1 and Sim2 are required for the correct targeting of mammillary body axons. Development. 2005; 132:5527–5537. [PubMed: 16291793]

Mastick GS, Easter SS Jr. Initial organization of neurons and tracts in the embryonic mouse fore- and midbrain. Dev Biol. 1996; 173:79–94. [PubMed: 8575640]

Mastick GS, Davis NM, Andrew GL, Easter SS Jr. Pax-6 functions in boundary formation and axon guidance in the embryonic mouse forebrain. Development. 1997; 124:1985–1997. [PubMed: 9169845]

Mastick GS, Farmer WT, Altick AL, Nural HF, Dugan JP, Kidd T, Charron F. Longitudinal axons are guided by Slit/Robo signals from the floor plate. Cell Adhes Migrat. 2010; 4:337–341.

Nguyen, Ba-Charvet KT.; Brose, K.; Marillat, V.; Kidd, T.; Goodman, CS.; Tessier-Lavigne, M.; Sotelo, C.; Chedotal, A. Slit2-Mediated chemorepulsion and collapse of developing forebrain axons. Neuron. 1999; 22:463–473. [PubMed: 10197527]

NIH-PA Author Manuscript

NIH-PA Author Manuscript

NIH-PA Author Manuscript

Nguyen-Ba-Charvet KT, Plump AS, Tessier-Lavigne M, Chedotal A. Slit1 and slit2 proteins control the development of the lateral olfactory tract. J Neurosci. 2002; 22:5473–5480. [PubMed: 12097499]

Nguyen-Ba-Charvet KT, Picard-Riera N, Tessier-Lavigne M, Baron-Van Evercooren A, Sotelo C, Chedotal A. Multiple roles for slits in the control of cell migration in the rostral migratory stream. J Neurosci. 2004; 24:1497–1506. [PubMed: 14960623]

Nural HF, Mastick GS. Pax6 guides a relay of pioneer longitudinal axons in the embryonic mouse forebrain. J Comp Neurol. 2004; 479:399–409. [PubMed: 15514979]

Plump AS, Erskine L, Sabatier C, Brose K, Epstein CJ, Goodman CS, Mason CA, Tessier-Lavigne M. Slit1 and Slit2 cooperate to prevent premature midline crossing of retinal axons in the mouse visual system. Neuron. 2002; 33:219–232. [PubMed: 11804570]

Rhee J, Mahfooz NS, Arregui C, Lilien J, Balsamo J, VanBerkum MF. Activation of the repulsive receptor Roundabout inhibits N-cadherin-mediated cell adhesion. Nat Cell Biol. 2002; 4:798–805. [PubMed: 12360290]

Ringstedt T, Braisted JE, Brose K, Kidd T, Goodman C, Tessier-Lavigne M, O'Leary DD. Slit inhibition of retinal axon growth and its role in retinal axon pathfinding and innervation patterns in the diencephalon. J Neurosci. 2000; 20:4983–4991. [PubMed: 10864956]

Ross LS, Parrett T, Easter SS Jr. Axonogenesis and morphogenesis in the embryonic zebrafish brain. J Neurosci. 1992; 12:467–482. [PubMed: 1371313]

Sundaresan V, Mambetisaeva E, Andrews W, Annan A, Knoll B, Tear G, Bannister L. Dynamic expression patterns of Robo (Robo1 and Robo2) in the developing murine central nervous system. J Comp Neurol. 2004; 468:467–481. [PubMed: 14689480]

Taylor JS. The early development of the frog retinotectal projection. Development Suppl. 1991; 2:95–104.

Tsuchiya R, Takahashi K, Liu FC, Takahashi H. Aberrant axonal projections from mammillary bodies in Pax6 mutant mice: possible roles of Netrin-1 and Slit 2 in mammillary projections. J Neurosci Res. 2009; 87:1620–1633. [PubMed: 19115401]

Wilkinson, D. In situ hybridization. Oxford: IRL Press; 1992.

Yeo SY, Little MH, Yamada T, Miyashita T, Halloran MC, Kuwada JY, Huh TL, Okamoto H. Overexpression of a slit homologue impairs convergent extension of the mesoderm and causes cyclopia in embryonic zebrafish. Dev Biol. 2001; 230:1–17. [PubMed: 11161558]

Yuan W, Zhou L, Chen JH, Wu JY, Rao Y, Ornitz DM. The mouse SLIT family: secreted ligands for ROBO expressed in patterns that suggest a role in morphogenesis and axon guidance. Dev Biol. 1999; 212:290–306. [PubMed: 10433822]

NIH-PA Author Manuscript
NIH-PA Author Manuscript
NIH-PA Author Manuscript

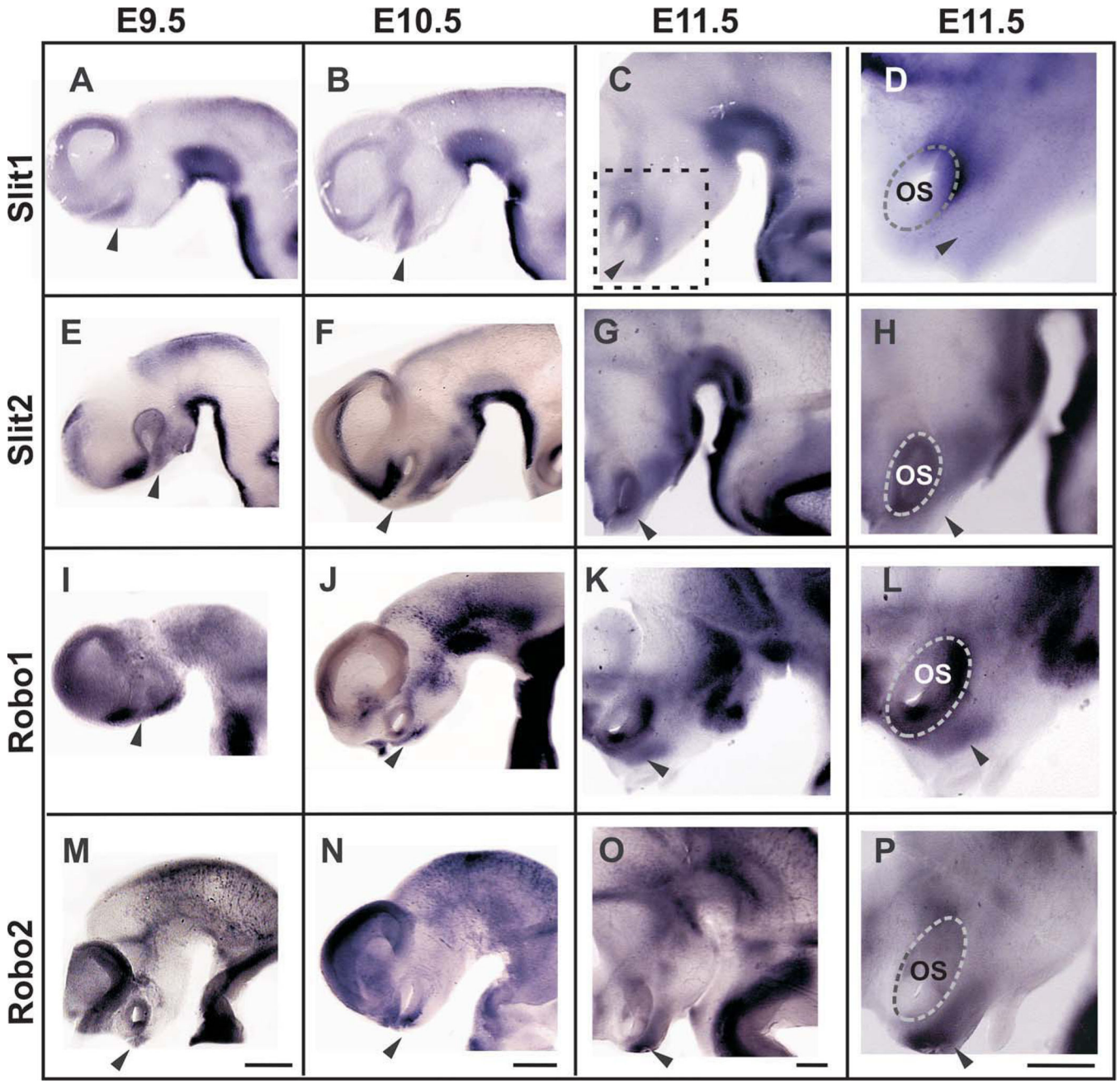

Fig. 1.

A–P: Expression patterns of *Slits* and *Robos* in mouse embryonic brains. Lateral views of the forebrain and midbrain (rostral is to the left). The approximate location of the nTPOC is indicated by arrowheads. The location of the higher magnification views shown in D, H, L, and P is indicated in C. Scale bars in each of the bottom panels applies to all micrographs of the column (200 μm in all).

NIH-PA Author Manuscript

NIH-PA Author Manuscript

NIH-PA Author Manuscript

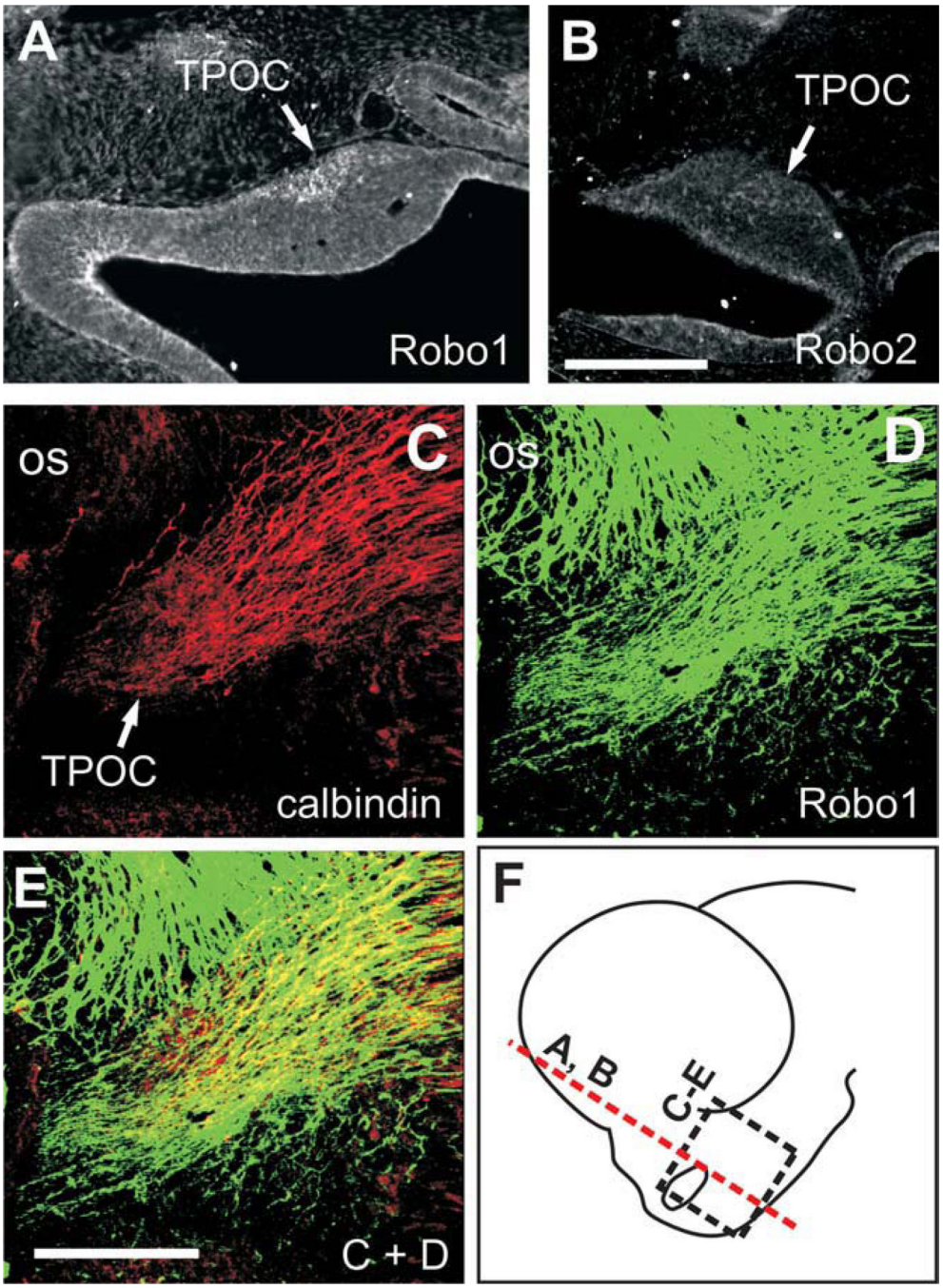

Fig. 2.

TPOC neurons express Robo proteins. **A,B**: Staining for Robo1 and Robo2 on coronal sections through the brain of E10.5 embryos. **C–E**: Whole-brain immunostaining of an E11.5 brain with calbindin and Robo1. **F**: Approximate location of sections in A and B (red dashed line) and of the field shown in C–E (black dashed-line rectangle). os, Optic stalk. Scale bars = 100 μm in B (applies to A,B); 100 μm in E (applies to C–E).

NIH-PA Author Manuscript
NIH-PA Author Manuscript
NIH-PA Author Manuscript

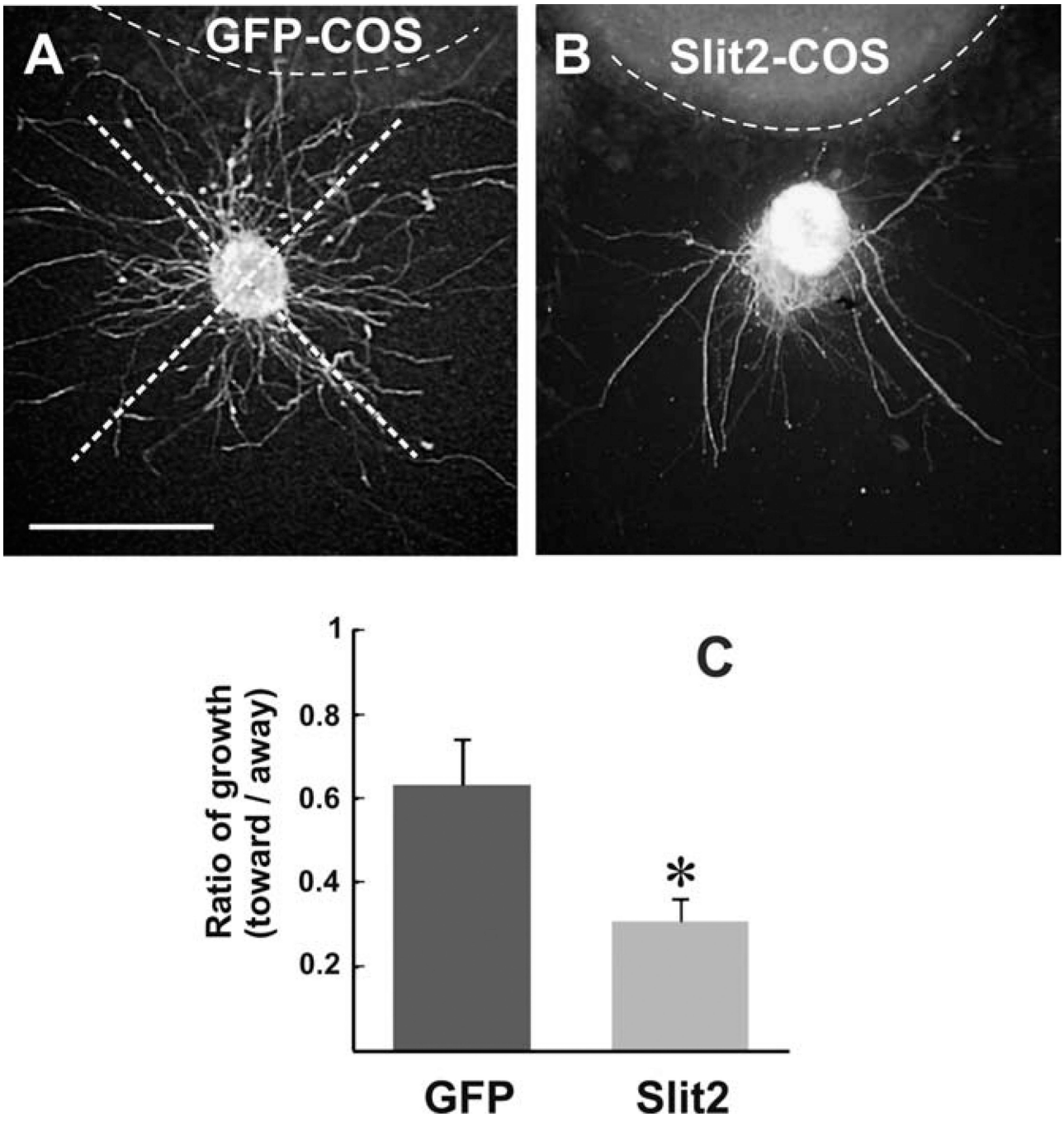

Fig. 3.

Slit2 inhibits TPOC axon growth in vitro. **A,B**: Explants from E10.5 embryos containing the nTPOC cultured in collagen gels exposed to COS cell aggregates transfected with a Slit2-myc (B) or a GFP expression vector (A) followed by β-tubulin III immunostaining. **C**: Quantification of neurite outgrowth within quadrants facing toward or away from the COS cell aggregate as shown in A. Graph shows the average ratio of toward/away growth (±SEM; n = 10 explants for GFP, n = 9 explants for Slit2). Explants had less neurite growth toward Slit2 aggregates than to control aggregates (*$P < 0.05$ by *t*-test). Scale bar = 100 μm.

NIH-PA Author Manuscript

NIH-PA Author Manuscript

NIH-PA Author Manuscript

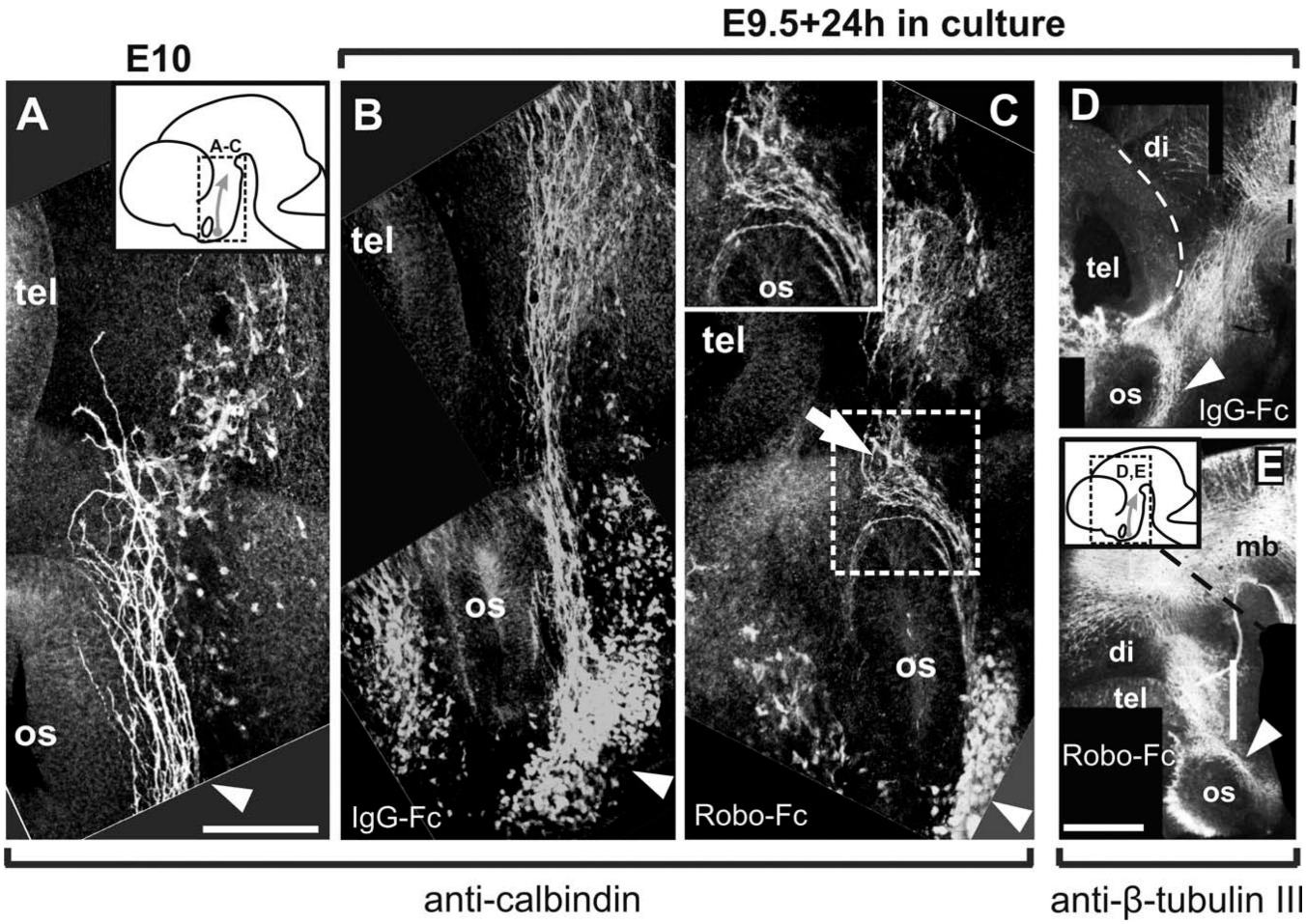

Fig. 4.

Impairing Robo function in cultured embryos causes alterations to TPOC projection. Calbindin immunostaining of the brain of E10 embryos allows visualization of the early stages of TPOC projection (**A**). E9.5 embryos were cultured for 24 hr in the presence of IgG-Fc protein (**B**) or in the presence of Robo1 and Robo2 Fc chimeras (**C**), followed by calbindin immunostaining. Approximate location of the brain region shown in A–C is indicated in the **inset** in A. The brains of embryos cultured with Fc control proteins (**D**) or with Robo-Fc chimeras (**E**) were immunostained for β-tubulin III. Region shown in D and E is indicated in the *inset* in E. tel, Telencephalon; mb, midbrain; hb, hindbrain; di, diencephalon; os, optic stalk. Scale bars = 100 μm in A (applies to A–C); 200 μm in E (applies to D,E).

NIH-PA Author Manuscript

NIH-PA Author Manuscript

NIH-PA Author Manuscript

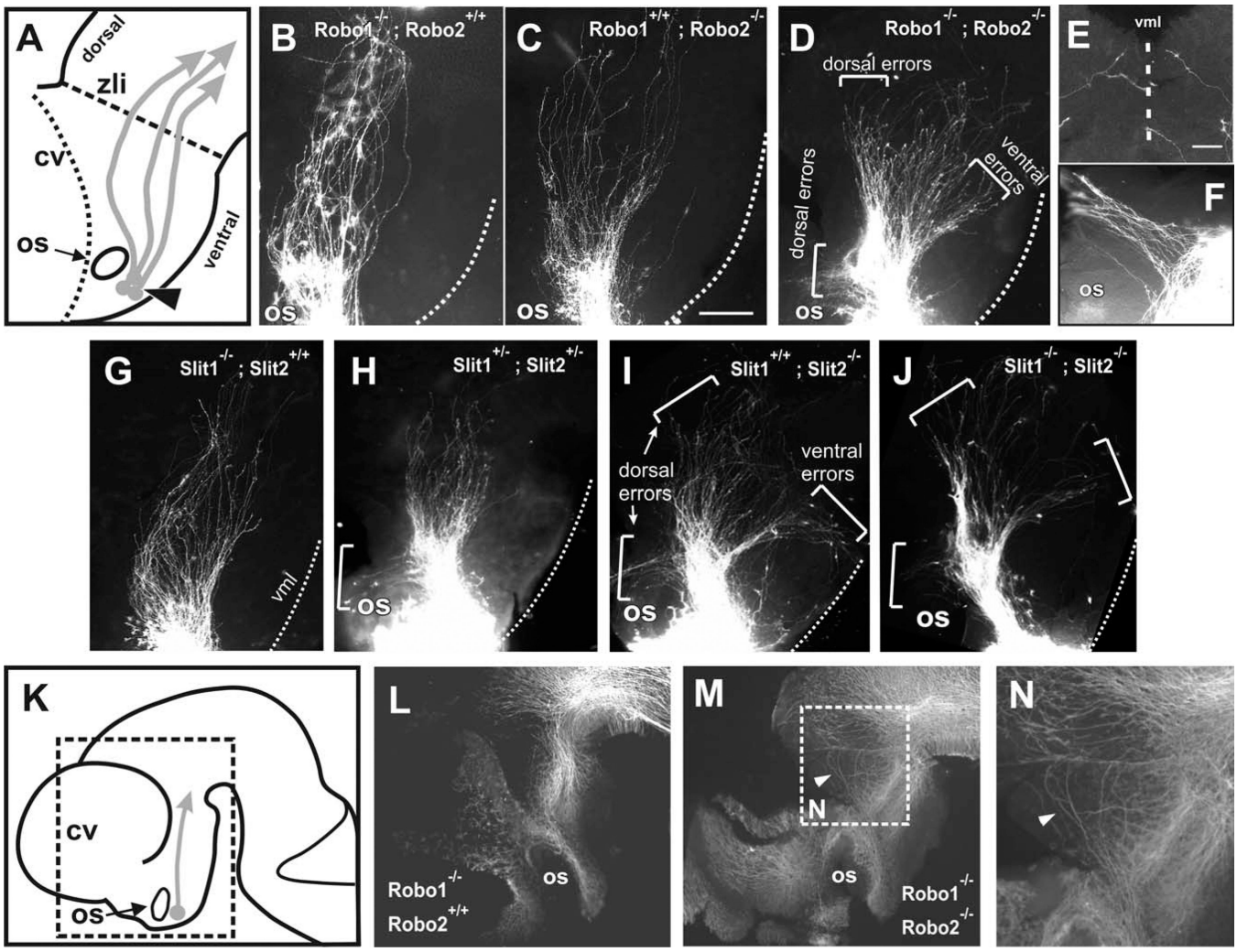

Fig. 5.

Loss of *Robo1-Robo2* and of *Slit1-Slit2* results in TPOC path-finding errors. DiI labeling of the TPOC in E10.5–E11 mouse embryos. **A**: Diagram of anterior forebrain (rostral is to the left) showing the normal TPOC trajectory (arrows) and the location of the DiI crystals for TPOC labelling (arrowhead). **B,C**: *Robo1* and *Robo2* single mutants have largely normal TPOC trajectories, although *Robo2* single mutants display deviations limited to a slight dorsal widening of the tract (C). **D**: In *Robo1/2* double mutants, TPOC axons make severe pathfinding errors, resulting in misprojection (brackets) or in expanded tracts. **E**: Ventral midline view of a *Robo1/2* double mutant brain showing bilaterally labelled axons aberrantly invading the ventral midline. **F**: High magnification of an embryo showing axons turning dorsally around the optic stalk. **G**: *Slit1*$^{-/-}$ mutants appear largely normal. **H**: *Slit1/Slit2* double heterozygotes have some axons turn (bracket) around the optic stalk, while most axons continue normal trajectories. **I**: *Slit2* mutants have a wider TPOC and axons wander both ventrally and dorsally (brackets; these errors were seen bilaterally in two of three analyzed of this genotype). **J**: *Slit1/Slit2* double mutants have extensive projection errors, similar to *Slit2* and *Robo1*; *Robo2* mutants. Control (**L**) and *Robo1/Robo2* double

NIH-PA Author Manuscript

NIH-PA Author Manuscript

NIH-PA Author Manuscript

mutants (**M,N**) were immunostained for β-tubulin III to reveal potential alterations to tracts other than the TPOC. Location of regions shown in L and M is indicated in **K**. Location of N is indicated in M. cv, Cerebral vesicles; os, optic stalk; zli, zona limitans intrathalamica; vml, ventral midline. Scale bars = 100 μm in C (applies to B–D,G–J); 200 μm for L,M; 50 μm in E (applies to E,F).